


Observation of giant gain and coupled parametric oscillations between four optical channels in cascaded four-wave mixing

J. P. Lopez, A. M. G. de Melo, D. Felinto, and J. W. R. Tabosa 

Departamento de Física, Universidade Federal de Pernambuco, 50670-901 Recife, PE, Brazil



(Received 17 April 2019; published 26 August 2019)

In this work, we explore both the internal and external atomic degrees of freedom to demonstrate the observation of giant gain and parametric oscillation in multiple four-wave mixing (FWM) processes in a sample of cold cesium atoms. We employ a standard backward FWM beam configuration to achieve parametric probe-beam gains exceeding 2000. This giant gain is accompanied by the generation of three other beams of equivalent power emitted along the directions satisfying the phase-matching conditions for multiple cascade forward and backward FWM triggered by the incident probe and the counterpropagating pumping beams. Moreover, we have also observed a simultaneous threshold for parametric oscillation of the four coupled optical fields with the pump intensity. These results point to an alternative pathway to generate multipartite correlated optical fields associated with long-lived atomic systems for applications in quantum information.

DOI: [10.1103/PhysRevA.100.023839](https://doi.org/10.1103/PhysRevA.100.023839)

I. INTRODUCTION

Optical parametric amplification, or the exchange of energy between different light fields mediated by an atomic medium, plays a fundamental role in the generation of classical and nonclassical light [1]. This phenomenon is usually governed by the second-order ($\chi^{(2)}$) or third-order ($\chi^{(3)}$) nonlinear susceptibility associated, respectively, with the three- and four-wave mixing (FWM) nonlinear processes. Forward FWM with gain factors on the order of 10 associated with strong intensity squeezing [2] is behind, for example, the generation of entangled images [3], with possible applications in the multiplexing of continuous-variable quantum communication protocols. With the addition of a cavity around the nonlinear medium, optical parametric oscillators (OPOs) based on three-wave mixing have found a wide range of applications in quantum information as well, with the notable achievement in recent years of large-scale entangled quantum states [4,5]. In most applications of quantum optics, the OPO works below its oscillation threshold. However, above-threshold OPOs have also been applied recently for the generation of multi-color hexapartite entanglement [6,7].

Optical parametric oscillation can actually be achieved even without a cavity, using phase conjugation to reflect waves inside a nonlinear medium. Since the first theoretical proposals for such mirrorless optical parametric oscillation (MOPO) based on three- and four-wave mixing [8,9], which occurred more than four decades ago, several experimental demonstrations of this phenomenon have been reported [10–12]. Specifically, in the case of FWM with two counterpropagating pumping beams, the generated photon pair propagates in opposite directions, thus providing the distributed feedback necessary for optical oscillation without the need of any

external cavity. FWM-based MOPO via electromagnetically induced resonance (EIT) was demonstrated in thermal rubidium vapors [13,14] and more recently also in cold rubidium atoms [15]. Previous work has also reported cavityless super-radiance [16] and MOPO [17] based on the atomic external degrees of freedom. In the previously mentioned MOPO studies, only two spatial modes are usually considered to be coupled. Nevertheless, it was also demonstrated that multi-mode MOPO can be achieved via multiple FWM processes in a sample of sodium thermal atoms [18–20], exploring the atomic internal degrees of freedom. In particular, in their four-wave parametric oscillation scheme the coupled-mode wave vectors and frequencies lead to Stokes and anti-Stokes modes shifted from the pump frequency by the sodium hyperfine splitting. Also, due to the much larger Doppler broadening, this multiple parametric oscillation depends critically on the position of the pump frequency inside the Doppler width, and EIT is crucial for canceling the absorption of the generated fields.

In this work, we present a demonstration of multiple parametric four-wave mixing in a sample of cold atoms exploring both the internal and external atomic degrees of freedom, where the restrictive conditions mentioned above are not required for the observation of MOPO. As a result, we report on the observation of extremely high values of saturated optical parametric gain (on the order of 2000) with a very narrow bandwidth (around 15 kHz) and moderate pump intensities (180 mW/cm² total). This gain on a probe beam is accompanied by simultaneous generation by the medium of three other beams of similar intensity. We measured a simultaneous oscillation threshold for the four fields, highlighting their fundamentally coupled nature.

II. EXPERIMENTAL SETUP AND RESULTS

Our basic configuration consists of two counterpropagating pumping beams (C_1 and C_2) with orthogonal linear

* Author to whom all correspondence should be addressed: tabosa@df.ufpe.br

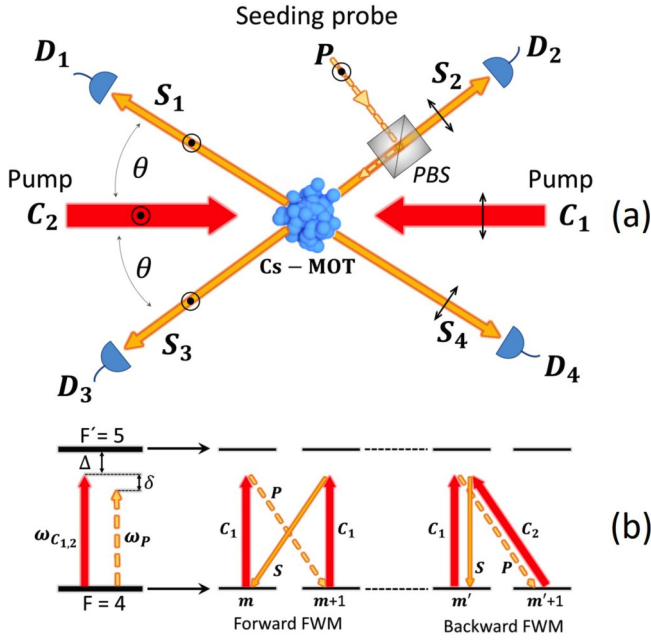


FIG. 1. (a) Simplified experimental beam configuration to observe multiple FWM processes. The two counterpropagating pumping beams (C_1 and C_2) with linear orthogonal polarizations and the seeding probe (P) orthogonally polarized to C_1 generate the four modes specified by S_1 , S_2 , S_3 , and S_4 , with the indicated polarizations and incident at different avalanche photodetectors (D). (b) Partial Zeeman levels associated with the cesium closed transition $6S_{1/2}, F = 4 \rightarrow 6P_{3/2}, F' = 5$, showing the interaction diagrams associated with forward and backward FWM processes. The pump frequencies are $\omega_{C_1} = \omega_{C_2} = \omega$, and the probe (P) frequency is $\omega_p = \omega - \delta$.

polarizations and a very weak seeding probe beam (P) with linear polarization orthogonal to that of the nearly copropagating pump beam, as depicted in Fig. 1(a). The two pump beams have the same frequency ω and wave vectors $\vec{k}_{C_2} = -\vec{k}_{C_1}$, while the seeding probe has frequency $\omega - \delta$ and wave vector \vec{k}_P . For such beam geometry interacting nearly in resonance with a Zeeman degenerate two-level system, several nonlinear third-order $\chi^{(3)}$ processes can occur. As examples, consider the two processes shown in the diagrammatic photon-atom interaction picture of Fig. 1(b), where the two signals S_1 and S_2 , with wave vectors $\vec{k}_{S_1} = 2\vec{k}_{C_1} - \vec{k}_P$ and $\vec{k}_{S_2} = -\vec{k}_P$, are generated, satisfying phase matching for $\theta \ll 1$ via nearly degenerate forward and backward FWM, respectively. In particular, coherent Bragg scattering associated with recoil-induced resonance (RIR), also contributes to the signal generated along the direction \vec{k}_{S_2} [21,22]. The polarization of the generated signals S_1 and S_2 is determined by the angular momentum selection rules, and it is specified in Fig. 1(a). If the efficiency of these FWM processes is sufficiently high, the generated signals S_1 and S_2 act as the new seeding beams to generate, via the same nonlinear processes, the signals S_3 and S_4 , with wave vectors $\vec{k}_{S_3} = -\vec{k}_{S_2}$ and $\vec{k}_{S_4} = -\vec{k}_{S_1}$ and the indicated polarizations in Fig. 1(a). Closing the feedback loop, the signals S_3 and S_4 couple parametrically with the pumping beams to generate again the S_1 and S_2 signals. As a result of these multiple cascading FWM processes, one can

obtain, in each generated mode, optical powers that exceed by a huge factor the power of the incident seeding beam. In the following, we describe the experimental apparatus and results.

In the experiment, we employed cold cesium atoms obtained from a conventional magneto-optical trap (MOT), with atomic clouds of approximately 1 mm diameter and an optical depth of 5, initially prepared in the higher hyperfine ground state $6S_{1/2}, F = 4$. The trapping and the repumping beams, as well as the MOT quadrupole magnetic field, are turned off during all measurements. We use a microwave spectroscopy technique to cancel any stray magnetic field, as described previously in [23,24]. The pump beams C_1 and C_2 have approximately the same diameter of 0.8 mm and are provided by an external cavity diode laser locked to a saturated absorption signal. They have their frequencies shifted by an acousto-optic modulator (AOM) detuned by about $\Delta = 6\Gamma$ ($\Gamma/2\pi = 5.2$ MHz) below the resonance frequency of the cesium closed transition $6S_{1/2}, F = 4 \rightarrow 6P_{3/2}, F' = 5$. The seeding probe P with a slightly smaller diameter is also obtained from the same laser, and its frequency can be scanned around the pump frequency by an independent AOM.

We used auxiliary beams to align the four avalanche photodetectors along the four symmetric directions making an angle of $\theta = 1^\circ$ with the pumping beams. The angle θ is determined by the incident seeding beam. The pumping and seeding beams are turned on for a period of 400 μs . For $\delta = 0$, in the insets of Fig. 2 we show the time evolution of each generated signal. As can be seen, after some tens of μs the generated signals start to build up, reaching approximately maxima values of the same order of magnitude. The time required to reach the stationary state decreases with increasing pumping beam intensity, and for longer excitation times all signal amplitudes show a slight reduction due to optical pumping, which removes the atoms from the interacting transition. For pumping beams with the same intensity of 90 mW/cm^2 and a seeding probe intensity of 10 $\mu\text{W}/\text{cm}^2$, we show in Fig. 2 the maximum signal amplitudes as a function of the probe-pump detuning $-\delta$ for the four generated signals. If we define the optical gain as the ratio between the generated intensity and the intensity of the incident seeding probe, these data correspond to a gain of about 1000. We should note that the four generated signals have approximately the same intensity. Furthermore, it is worth mentioning that under specific conditions, we have observed maximum gain exceeding 2000. Indeed, we observed that this measured giant gain saturates strongly for increasing probe beam intensity, in a manner similar to gain saturation in conventional lasers.

III. EXPERIMENTAL ANALYSIS AND DISCUSSIONS

As theoretically discussed in [21] and experimentally observed in [25], for the above polarization configuration the probe transmission spectrum can have contributions from different mechanisms associated with Raman and parametric FWM processes involving either the internal or the external atomic degrees of freedom. This $\text{lin} \perp \text{lin}$ pump polarization configuration gives rise to Sisyphus cooling and to the creation of vibrational levels for atoms localized in the potential wells of the associated optical lattice, and to the corresponding

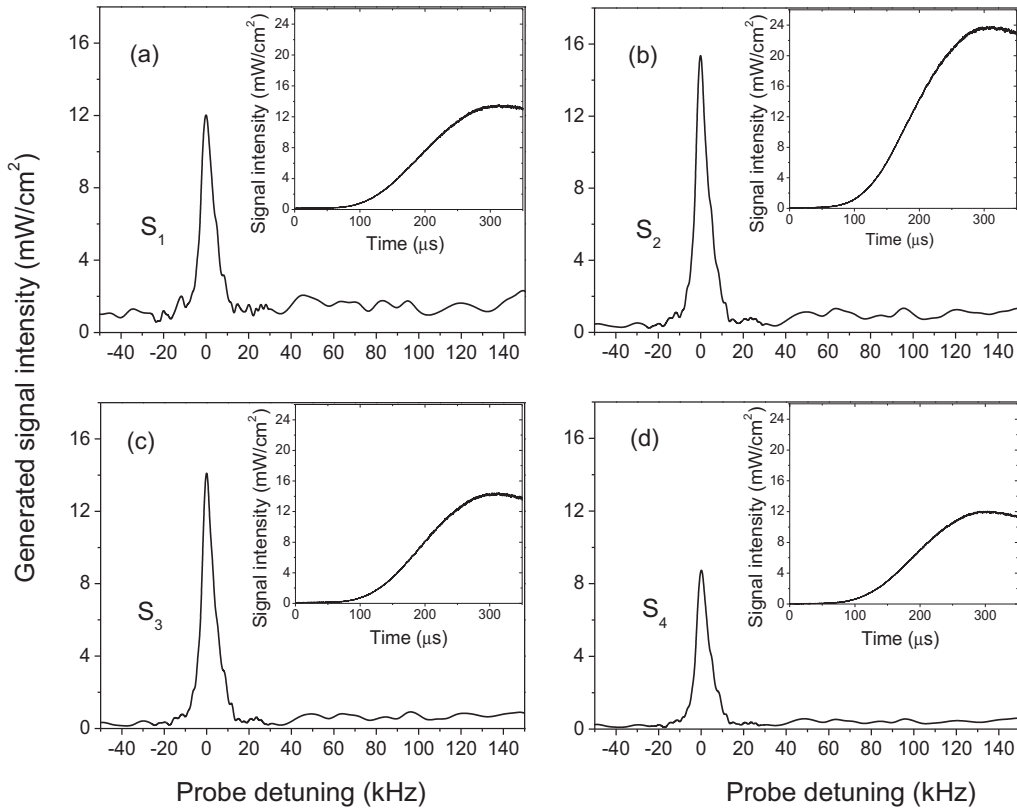


FIG. 2. Measured signal spectrum as a function of the probe detuning, $\omega_p - \omega$, corresponding to each generated mode, as indicated in each frame. Inset: Time evolution of the amplitude of each generated signal, for $\delta = 0$, after turning on the incident beams at $t = 0$.

Raman absorption and gain involving these vibrational levels [26–28]. At the same time, the counterpropagating pump C_2 and the incident probe can also give rise to RIR as well as to the associated FWM via the Bragg scattering process. The present polarization configuration can also produce Raman gain and absorption involving the internal Zeeman states with different populations [29,30].

Thus, to better understand the observed gain mechanism, we have measured the spectrum of each generated signal, under the same experimental conditions as in Fig. 2, at different times after the turning on of the beams, as shown in Fig. 3. For short times ($t_0 \sim 64 \mu\text{s}$), the probe transmission spectrum reveals an absorption and gain that have mainly a structure associated with Raman transitions involving the internal Zeeman levels. The corresponding width of the dispersive feature of the probe transmission spectrum, of the order of 100 kHz, is consistent with the minimum spread in Zeeman shifts we have measured by the μ -wave spectroscopy technique employed for cancellation of the magnetic field. As it takes some time for the atoms to populate the vibrational levels as well as to create the density grating responsible for the generation of the RIR signals, we should expect a time delay for these mechanisms to manifest themselves. Therefore, only for later times ($t_0 \sim 100 \mu\text{s}$) can we see the appearance of the narrower central peak associated with the RIR process, having a width of the order of 15 kHz [25,28], which then evolves according to the coupled cascading FWM to reach a steady state where all the generated modes have approximately the same intensity for much later times ($t_0 \sim 300 \mu\text{s}$).

In another series of measurements, we recorded the probe beam transmission for different values of the intensity of the counterpropagating pumping beam C_2 , keeping the intensity

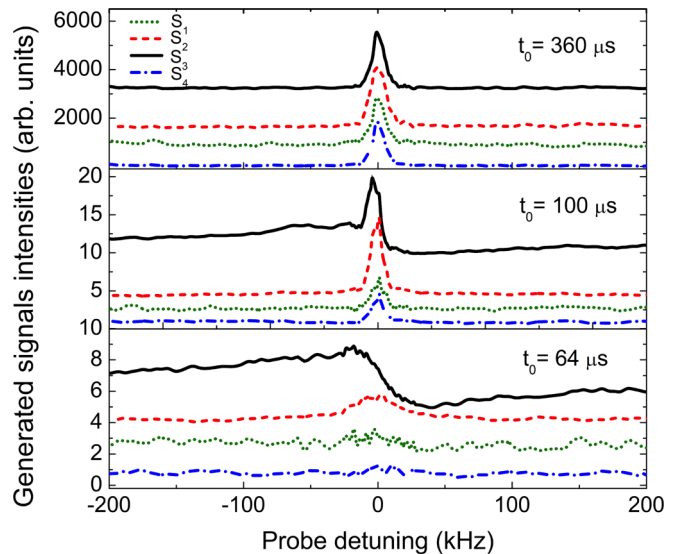


FIG. 3. Time evolution of the probe transmission and the FWM spectra recorded in different times (t_0) after the turning on of the incident beams, as indicated in each frame. The curves were shifted vertically in each frame for better visualization, but the vertical scales determine the relative amplitudes between them.

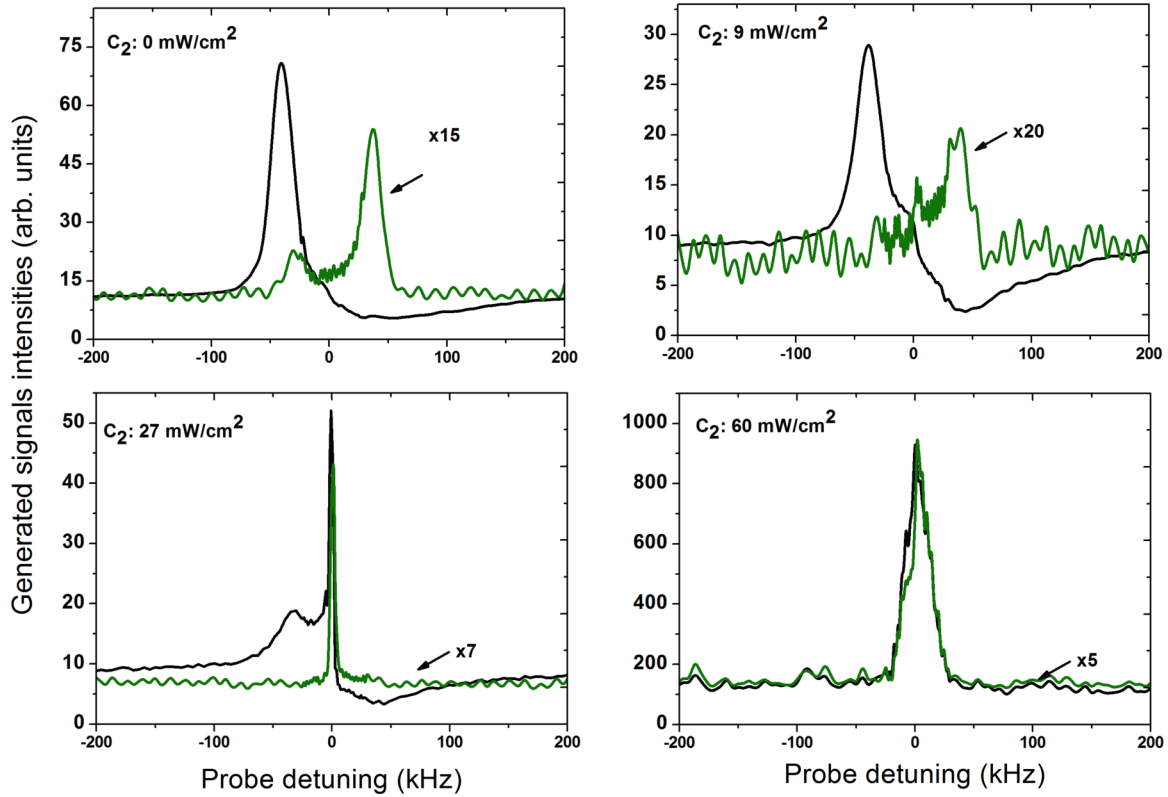


FIG. 4. Probe transmission (S_3) (black) and forward FWM (S_1) (green) spectra for different values of the pumping intensity C_2 and for a fixed intensity of the pumping beam C_1 equal to 60 mW/cm^2 , taken at stationary regime ($t_0 \sim 300 \mu\text{s}$).

of the C_1 beam fixed at 60 mW/cm^2 . As shown in Fig. 4(a), for zero intensity of the C_2 pump, we obtain the well-known dispersive line shape showing absorption and gain in the probe transmission spectrum [29,30]. We have also recorded the spectrum of the associated forward FWM signal, shown by the green curve. We note that, for this particular situation, this is the only allowed FWM process. However, for increasing values of the C_2 pump intensity, the transmission spectrum evolves with the simultaneous generation of the corresponding backward FWM signals, as shown in Figs. 4(b) and 4(c), with the formation of the central narrow peak associated with the RIR phenomenon. Finally, for higher C_2 intensities all four modes are generated, leading to a constructive interference around $\delta = 0$ and to sustained oscillation through the mentioned cascade multiple FWM processes producing macroscopic signals in all four modes with comparable intensities. We have verified experimentally that the appearance of the narrow gain peak in the probe transmission spectrum is accompanied by the simultaneous generation of the FWM signals in the other three modes, and that the gain reaches its maximum when the two pumping intensities are equal.

Finally, in Fig. 5 we present the dependence of each generated signal intensity with the common intensity of the pumping beams. This result clearly reveals a threshold behavior for this coupled parametric amplification. We have also verified experimentally an optical density threshold value of about 3 for this gain mechanism. Moreover, for sufficiently high pumping beam intensity we have observed that the system builds up spontaneously in self-oscillation without the need of any seeding beam. As this self-oscillation can occur in

many different spatial modes existing inside a cone around the pumping beam, the competition and coupling between these modes should induce fluctuations in time for the intensity measured in each detector, a fact we have observed experimentally.

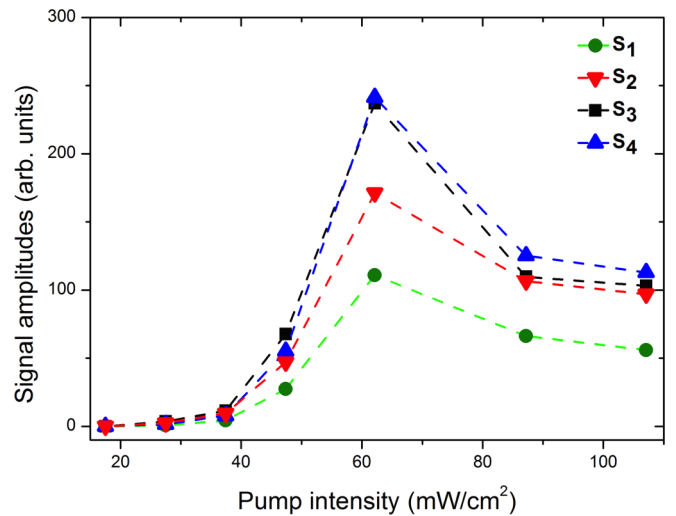


FIG. 5. Dependence of the amplitude of the generated signals as a function of the common intensity of the pumping beams, measured at $t_0 \sim 300 \mu\text{s}$, revealing a threshold behavior with a threshold pump intensity of about 40 mW/cm^2 . We attribute the different relative amplitudes for the corresponding signals in Fig. 2 to their high sensibility to alignment over the ensemble and on the detectors.

IV. CONCLUSIONS

In summary, we have demonstrated experimentally the observation of giant gain (up to 2000) and self-oscillation via multiple cascading parametric FWM in a sample of cold cesium atoms for moderate intensities of the pumping beams. We have monitored the time evolution of the various mechanisms responsible for the generation of several FWM processes, and we verified experimentally that the main contribution comes from processes associated with the RIR phenomenon. Furthermore, we believe that we have found a very promising system to investigate a branch of interesting

quantum physical phenomena, such as, for example, multi-mode quantum correlations, and storage and multiplexing of optical information. Indeed, we are currently investigating the use of this mechanism for light storage and for the production of high-intensity quantum correlated beams.

ACKNOWLEDGMENTS

This work was supported by the Brazilian grant agencies CNPq (Conselho Nacional de Desenvolvimento Científico e Tecnológico) and FACEPE (Fundação de Amparo à Ciência e Tecnologia do Estado de Pernambuco).

-
- [1] M. O. Scully and M. S. Zubairy, *Quantum Optics* (Cambridge University Press, Cambridge, 1997).
 - [2] C. F. McCormick, A. M. Marino, V. Boyer, and P. D. Lett, *Phys. Rev. A* **78**, 043816 (2008).
 - [3] V. Boyer, A. M. Marino, R. C. Pooser, and P. D. Lett, *Science* **321**, 544 (2008).
 - [4] S. Yokoyama, R. Ukai, S. C. Armstrong, C. Sornphiphatpong, T. Kaji, S. Suzuki, J.-i. Yoshikawa, H. Yonezawa, N. C. Menicucci, and A. Furusawa, *Nat. Photonics* **7**, 982 (2013).
 - [5] M. Chen, N. C. Menicucci, and O. Pfister, *Phys. Rev. Lett.* **112**, 120505 (2014).
 - [6] A. S. Coelho, F. A. S. Barbosa, K. N. Cassemiro, A. S. Villar, M. Martinelli, and P. Nussenzveig, *Science* **326**, 823 (2009).
 - [7] F. A. S. Barbosa, A. S. Coelho, L. F. Muñoz-Martínez, L. Ortiz-Gutiérrez, A. S. Villar, P. Nussenzveig, and M. Martinelli, *Phys. Rev. Lett.* **121**, 073601 (2018).
 - [8] S. E. Harris, *Appl. Phys. Lett.* **9**, 114 (1966).
 - [9] A. Yariv and D. M. Pepper, *Opt. Lett.* **1**, 16 (1977).
 - [10] D. M. Pepper, D. Fekete, and A. Yariv, *Opt. Lett.* **33**, 41 (1978).
 - [11] J. R. R. Leite, P. Simoneau, D. Bloch, S. L. Boiteux, and M. Ducloy, *Europhys. Lett.* **2**, 747 (1986).
 - [12] M. Pinar, D. Grandclement, and G. Grynberg, *Europhys. Lett.* **2**, 755 (1986).
 - [13] A. S. Zibrov, M. D. Lukin, and M. O. Scully, *Phys. Rev. Lett.* **83**, 4049 (1999).
 - [14] S. S. Sahoo, S. S. Pati, and A. K. Mohapatra, *Phys. Rev. A* **98**, 063838 (2018).
 - [15] Y. Mei, X. Guo, L. Zhao, and S. Du, *Phys. Rev. Lett.* **119**, 150406 (2017).
 - [16] J. A. Greenberg and D. J. Gauthier, *Phys. Rev. A* **86**, 013823 (2012).
 - [17] A. Schilke, C. Zimmermann, P. W. Courteille, and W. Guerin, *Nat. Photon.* **6**, 101 (2012).
 - [18] K. Motomura, M. Tsukamoto, A. Wakiyama, K.-i. Harada, and M. Mitsunaga, *Phys. Rev. A* **71**, 043817 (2005).
 - [19] K.-i. Harada, M. Ogata, and M. Mitsunaga, *Opt. Lett.* **32**, 1111 (2007).
 - [20] K.-i. Harada, N. Hayashi, K. Mori, and M. Mitsunaga, *J. Opt. Soc. Am. B* **25**, 40 (2008).
 - [21] J. Guo, *Phys. Rev. A* **49**, 3934 (1994).
 - [22] J. Greenberg and D. J. Gauthier, *Europhys. Lett.* **98**, 24001 (2012).
 - [23] L. Veissier, Thèse de Doctorat, Laboratoire Kastler Brossel, Université Pierre et Marie Curie, 2013.
 - [24] A. J. F. de Almeida, M.-A. Maynard, C. Banerjee, D. Felinto, F. Goldfarb, and J. W. R. Tabosa, *Phys. Rev. A* **94**, 063834 (2016).
 - [25] J. Greenberg, B. L. Schmittberger, and D. J. Gauthier, *Opt. Express* **19**, 22535 (2011).
 - [26] P. Verkerk, B. Lounis, C. Salomon, C. Cohen-Tannoudji, J.-Y. Courtois, and G. Grynberg, *Phys. Rev. Lett.* **68**, 3861 (1992).
 - [27] M. Brzozowska, T. M. Brzozowski, J. Zachorowski, and W. Gawlik, *Phys. Rev. A* **73**, 063414 (2006).
 - [28] J. P. Lopez, A. J. F. de Almeida, D. Felinto, and J. W. R. Tabosa, *Opt. Lett.* **42**, 4474 (2017).
 - [29] J. W. R. Tabosa, G. Chen, Z. Hu, R. B. Lee, and H. J. Kimble, *Phys. Rev. Lett.* **66**, 3245 (1991).
 - [30] D. Grison, B. Lounis, C. Salomon, J. Y. Courtois, and G. Grynberg, *Europhys. Lett.* **15**, 149 (1991).